SURAT TUGAS
Nomor: 923-R/UNTAR/PENELITIAN/III/2024

Rektor Universitas Tarumanagara, dengan ini menugaskan kepada saudara:

1. **ANIEK PRIHATININGSIH, Ir., M.M.**
2. **ALI ISKANDAR, S.T., M.T**

Untuk melaksanakan kegiatan penelitian/publikasi ilmiah dengan data sebagai berikut:

Judul	:	Dynamic pore water pressure in saturated soil due to turbine engine?s vibration
Nama Media	:	The Third International Conference of Construction, Infrastructure, and Materials (ICCIM 2023)
Penerbit	:	EDP Sciences
Volume/Tahun	:	429/04010/2023
URL Repository	:	https://www.e3s-conferences.org/articles/e3sconf/abs/2023/66/e3sconf_iccim2023_04010/e3sconf_iccim2023_04010.html

Demikian Surat Tugas ini dibuat, untuk dilaksanakan dengan sebaik-baiknya dan melaporkan hasil penugasan tersebut kepada Rektor Universitas Tarumanagara

11 Maret 2024
Rektor

Prof. Dr. Ir. AGUSTINUS PURNA IRAWAN

Print Security : 5225562d8ae27adb71e984eff3b440c6

Jl. Letjen S. Parman No. 1, Jakarta Barat 11440
P: 021 - 5695 8744 (Humas)
E: humas@untar.ac.id

Lembaga

- Pembelajaran
- Kemahasiswaan dan Alumni
- Penelitian & Pengabdian Kepada Masyarakat
- Penjaminan Mutu dan Sumber Daya
- Sistem Informasi dan Database

Fakultas

- Ekonomi dan Bisnis
- Hukum
- Teknik
- Kedokteran
- Psikologi
- Teknologi Informasi
- Seni Rupa dan Desain
- Ilmu Komunikasi
- Program Pascasarjana

Dynamic pore water pressure in saturated soil due to turbine engine's vibration

Aniek Prihatiningsih[1], *Ali* Iskandar[1], and *Veronica*[1*]

[1]Undergraduate Program of Civil Engineering, Universitas Tarumanagara, Jl. Letjen S. Parman No. 1, Jakarta, Indonesia

Abstract. The turbine engine that is operating will generate vibrations that are transmitted by the foundation into the soil layer. This causes the pore water pressure in the soil to increase, which causes the shear strength of the soil to decrease and can reduce the carrying capacity of the soil as a foundation resting place, which results in a reduced bearing capacity of the foundation as well. The pore water pressure in the soil consists of static pore water pressure and excess pore water pressure. Static pore water pressure is hydrostatic pressure that depend on Ground Water Level (GWL), while excess pore water pressure is the pore water pressure that occurs due to changes in undrained soil stress. Therefore, a study was conducted on the effect of gas turbine engine vibration on pore water pressure in sand and clay soils with a depth of 8,5 m (fine to coarse sand), 10,5 m (silty clay), and 12,5 m (medium to coarse sand). From the research results, the value of the pore water pressure ratio for each layer of soil was 0,32, 0,02, and 0,49, which can reduce the bearing capacity of the pile, especially in sandy soils and if the value is greater than one, it can be concluded that the soil has the potential for liquefaction.

1 Introduction

The operating turbine machine will generate vibrations that are transmitted by the foundation surrounding the soil layer. This causes the pore water pressure in the soil to increase, which causes the shear strength of the soil to decrease and can reduce the carrying capacity of the soil as a foundation resting place, which results in a reduced bearing capacity of the foundation as well.

Pore water pressure itself has the meaning of water pressure contained in the soil pores. The pore water pressure in the soil consists of static pore water pressure and excess pore water pressure. Static pore water pressure is the pore water pressure when the soil is stable, while excess pore water pressure is the pore water pressure that occurs due to changes in undrained soil stress. In addition, there is also an active pore water pressure, which in saturated soil has the same value as the pore water pressure ($P_{active} = P_{water}$) [1].

Generally, the pore water pressure in the soil is negative (compressive). However, due to capillary forces or undrained unloading, the pore water pressure can become positive (suction) [2]. In Fig. 1, the pore water pressure is positive (suction) in the soil above the Ground Water Level (GWL) and negative in the soil under the GWL.

An increase in pore water pressure occurs in dynamic soils due to back-and-forth vibrations that cause water to not be able to pass through the soil pores quickly so that excess pore water pressure dissipation does not occur. Turbine engines as cyclic loads also have the potential to cause soil to liquefy. Symptoms occur in saturated sand soils with moderate to fine gradations [3]. Liquefaction potential is evaluated using excess pore water pressure [4]. Seed and Lee (1996) define the initial liquefaction as the point where the increase in pore pressure is equal to the initial effective confining pressure (when $u_{excess} = \sigma_3'$ or the pore water pressure ratio $r_u = u_{excess}/\sigma_3' = 1{,}0$) [4].

The effective confining pressure can be calculated using the following Equation 1.

$$\sigma_3' = k_0 \times \gamma_{sat} \times H \quad (1)$$

Based on the laboratory test results in Fig. 2, it can be concluded that the denser soil will need more number of cyclic load to reach the maximum pore water pressure excess ratio. It can also be seen that in loose sand, initial liquefaction is reached ($r_u = 1{,}0$) in only 10 cycles. Meanwhile, in dense sand, the initial liquefaction is not achieved after 17 cycles because it takes thousands of cycles with a low shear stress amplitude to reach the initial liquefaction.

The relationship between cyclic shear stress, density, and the number of liquefaction failure cycles can be depicted in laboratory cyclic strength curves as shown in Fig. 3.

Therefore, in this study, a numerical analysis based on finite element pore water pressure was carried out in saturated soils, both in clay soils and sandy soils, in dynamic soils due to the turbine engine's vibration.

*Corresponding author: veronica.325190065@stu.untar.ac.id

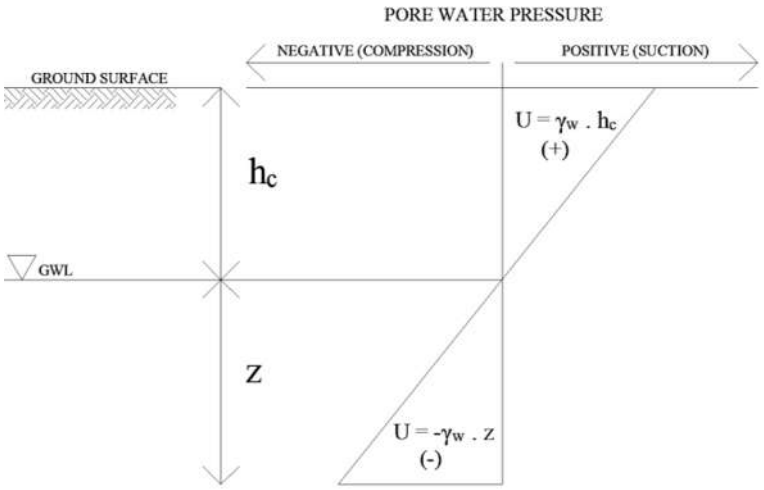

Fig. 1. Graphic of pore water pressure.

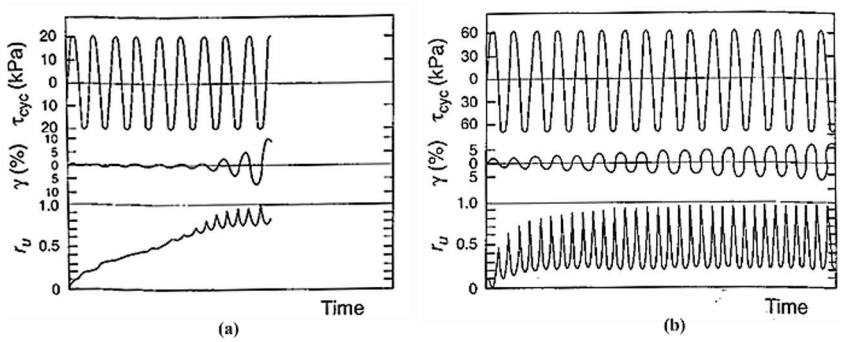

Fig. 2. Result of simple shear test on isotropically consolidated specimens of: (a) loose sand (DR = 47%); (b) dense sand (DR = 75%) [2].

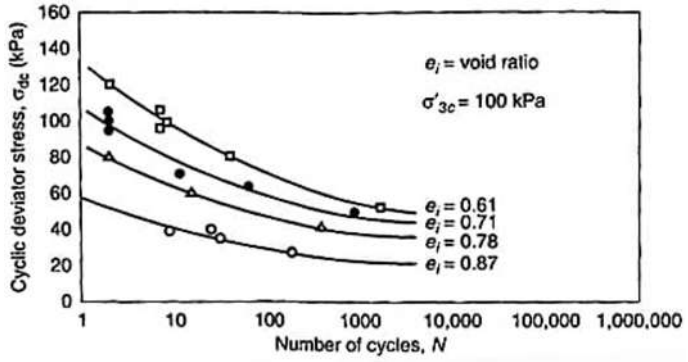

Fig. 3. Cyclic stress required for initial liquefaction and 20 % isotropically consolidated axial strain in triaxial specimens in Sacramento River sands (After Seed and Lee, 1965) [2].

1.1 Pile capacity

Decourt (1995) developed a more comprehesive correlation for calculating end bearing capacity with SPT value as follows Equation 2 [5].

$$Q_p = \sum A_p K_b \overline{N_b} \quad (2)$$

where A_p = pile toe area, $\overline{N_b}$ = average SPT value around pile toe, K_b = base factor given in Table 1.

Coyle and Castello (1981) give the Equation 3 for calculating skin capacity of foundation [6].

$$Q_s = \sum A_s f \quad (3)$$

Table 1. Base factor (K_b) [5].

Soil Type	Displacement Piles	Non-Displacement Piles
Sand	325	165
Sandy Silt	205	115
Clayey Silt	165	100
Clay	100	80

The unit friction resistance (f_s) can be estimated using the following Equations 4-6.

- Sand (β Method)

$$f = \beta\overline{\sigma'_o} \quad (4)$$

$$\beta = K\tan\delta' \quad (5)$$

- Clay (α Method)

$$f = \alpha c_u \quad (6)$$

where A_s = pile embedded shaft area, f = unit friction resistance, K = effective earth pressure coefficient, $\overline{\sigma'_o}$ = average effective vertical stress, δ' = soil-pile friction angle, α = empirical adhesion factor given in Table 2, c_u = undrained shear strength.

Table 2. Variation of α [6].

c_u/P_a	α
<0.1	1.00
0.2	0.92
0.3	0.82
0.4	0.74
0.6	0.62
0.8	0.54
1.0	0.48
1.2	0.42
1.4	0.40
1.6	0.38
1.8	0.36
2.0	0.35
2.4	0.34
2.8	0.35

Table **3** with the Mohr-Coulomb material model.

Specifications and machine foundation modeling data to be used for finite element modeling are shown in Tables 4-5.

The illustrations of the machine foundation structure to be modeled are shown in Fig. 4-5.

2.2 Dynamic loads

There are two kinds of foundation loading, static loads and dynamic loads. The static load is in the form of a turbine engine with a size of 13 m × 5.3 m × 5.5 m and a weight of 4,876 kN. Meanwhile, for dynamic loads, dynamic parameters are used in the form of a damping ratio value of 0.22 % which is obtained as a result of the piling activity of the foundation [7] with a load in the form of vertical displacement on the pile head results of the Pile Driving Analyzer (PDA) test in Table 6 and the pile head displacement graph in Fig. 6.

In addition, there is also a dynamic load on the turbine engine itself in the form of harmonic vibration of 10.3005 kN/s and a vibration frequency of 50 H_z.

2 Methodology

2.1 Soils and foundation structure modeling

The first thing to do is collect soil parameter data with GWL at a depth of 6.85 m. For modeling in finite element applications, soil parameters are used as shown in

Table 3. Soil parameters.

Parameters	Depth (m)			
	0-9	**9-11.55**	**11.55-15**	**15-30**
Soil Classifi-cation	Sand	Clay	Sand	Sand
Drainage Type	Undrained (A)	Undrained (A)	Undrained (A)	Undrai-ned (A)
γ_{unsat} (kN/m^3)	21	17	17	21
γ_{sat} (kN/m^3)	22	18	20	22
E' (kPa)	93,278	18,090	50,366	67,200
ν'	0.3	0.2	0.25	0.3
E_{oed} (kPa)	125,566	20,100	60,439	90,461
c' (kPa)	-	18	-	-
G (kPa)	35,876	7,537	20,146	25,846
ϕ' (°)	38	14	38	41
R_{inter}	1	0,5	1	1
K_0	0.3912	1	0.3912	0.3439
k (m/day)	0.5142	4.75×10^{-3}	0.5142	0.5142

3 Result and discussion

3.1 Pore water pressure analysis

Pore water pressure analysis was carried out on saturated soil with 10 cm from the outermost pile skin in the y direction at a depth of 8.5 m (fine to coarse sand), 10.5 m (silty clay), and 12.5 m (medium coarse sand) that can be seen in Fig. 7. Following that, it is determined whether the pore water pressure at that depth is suction or pressure, and its effect on the stability of the bearing capacity of the turbine engine foundation. The results of the analysis are the dynamic soil pore water pressure at the dynamic loading phase with a time interval of 5 s and the fading phase with a time interval of 0.5 s.

The results of calculating the pore water pressure from the finite element modeling for each soil layer are as follows Fig. 8-13.

Based on Fig. 8, it can be interpreted that at a depth of 8.5 m, the excess pore water pressure is positive, which means suction. Meanwhile, at a depth of 10.5 m and 12.5 m, based on Fig. 10 and Fig. 12, the excess pore water pressure is negative, which means compression. Based on Fig. 11 and Fig. 13,the increased value of active pore water pressure at a depth of 10.5 m is -40.79 kPa and at a

depth of 12.5 m is -101.33 kPa, which means that the deeper the soil layer, the compressive active pore water pressure will be greater. The active pore water pressure at the point under consideration and the static pore water pressure can be plotted onto a graph of pore pressure vs. depth as in
Fig. 14.

Table 4. Pile cap specification.

Parameters	Value
Dimensions	
P_{pc} (m)	15
L_{pc} (m)	7.3
T_{pc} (m)	2
Material Model	Linear elastic
Spesification	
Drainage Type	Non-porous
γ_{unsat} (kN/m^3)	24
e_0	0.5
f'$_c$ (MPa)	30 (assumption)
E (kPa)	25,742,960
ν'	0.1
G (kPa)	11,701,346
E_{od} (kPa)	26,328,027

Table 5. Pile group spesification.

Parameters	Value
Pile Group Dimensions	
n (pile)	8
S (m)	3
L_g (m)	9.6
B_g (m)	3.6
Spesification	
E (kPa)	33,892,182
γ (kN/m^3)	24
Beam Type	Predefined
Predefine Beam Type	Circular Tube
Diameter (m)	1
Wall Thickness (mm)	100
Axial Skin Resistance	
$T_{skin,start,max}$ (kN)	203
$T_{skin,end,max}$ (kN)	203
Base Resistamce	
F_{max} (kN)	4,212

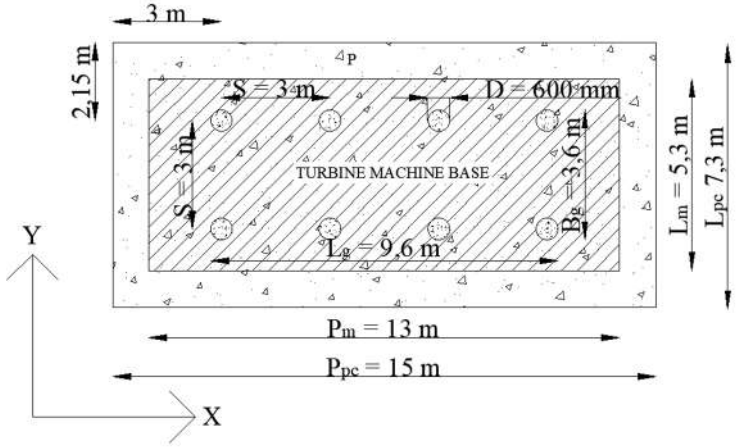

Fig. 4. Top view of machine foundation layout.

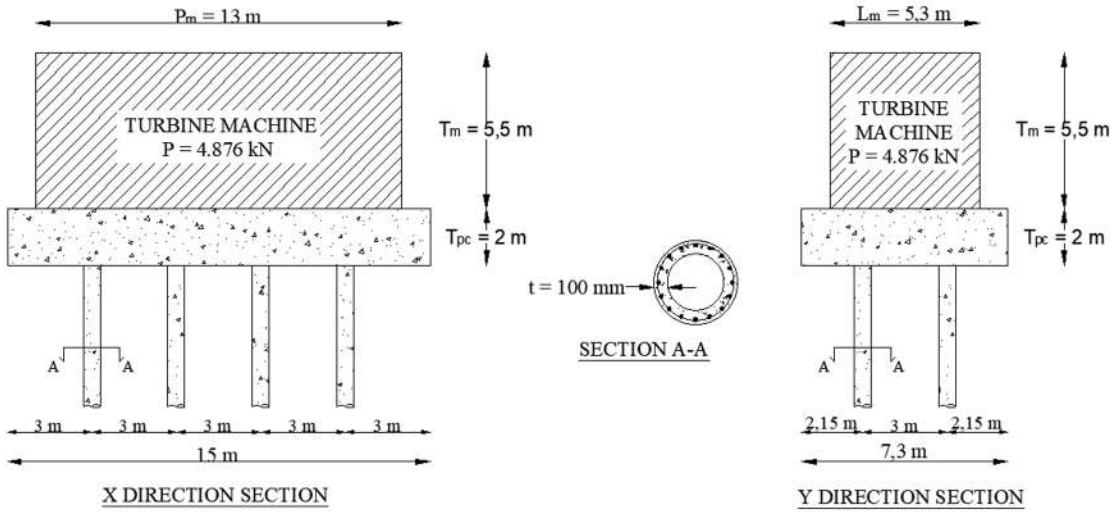

Fig. 5. Side view of machine foundation layout.

Table 6. Dynamic time (t) vs. displacement (S) when pile driving.

t (s)	S (m)
0	0
0.00512	0
0.01024	0.015
0.01536	0.0135
0.02048	0.009
0.0256	0.0059
0.04608	0.006

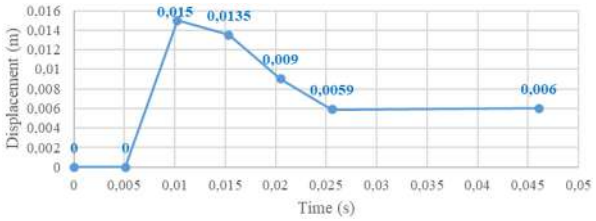

Fig. 6. Vertical displacement of pile head.

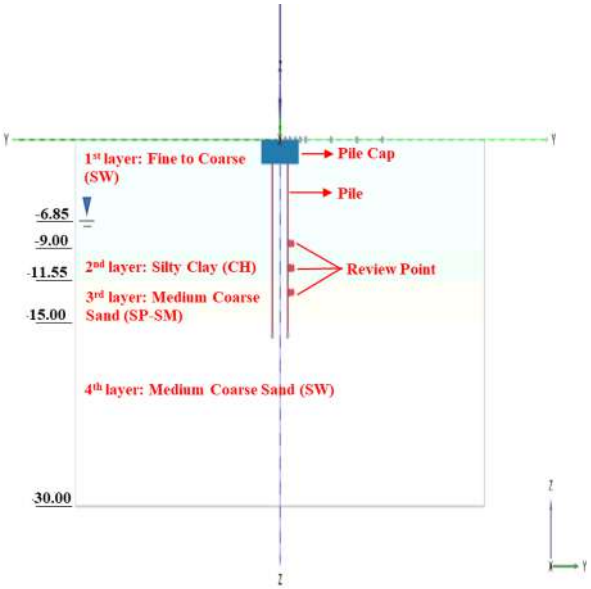

Fig. 7. Review points per layer.

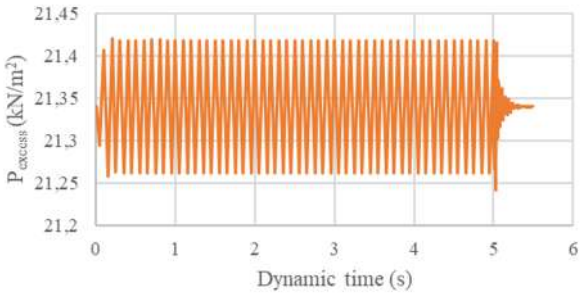

Fig. 8. Excess pore water pressure at a depth of 8.5 m.

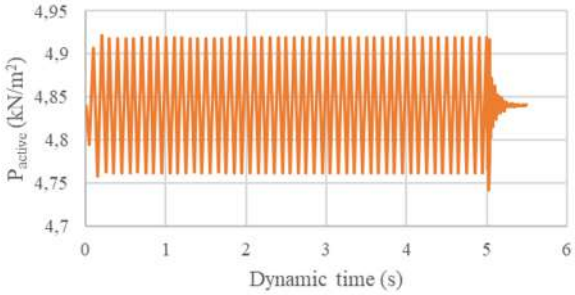

Fig. 9. Active pore water pressure at a depth of 8.5 m.

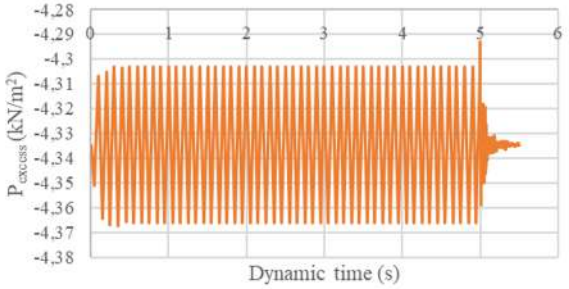

Fig. 10. Excess pore water pressure at a depth of 10.5 m.

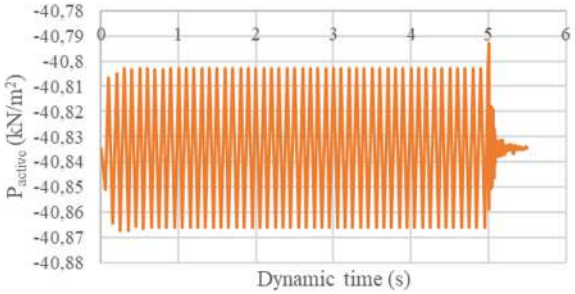

Fig. 11. Active pore water pressure at a depth of 10.5 m.

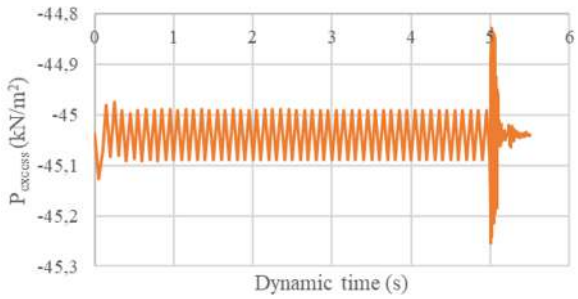

Fig. 12. Excess pore water pressure at a depth of 10.5 m.

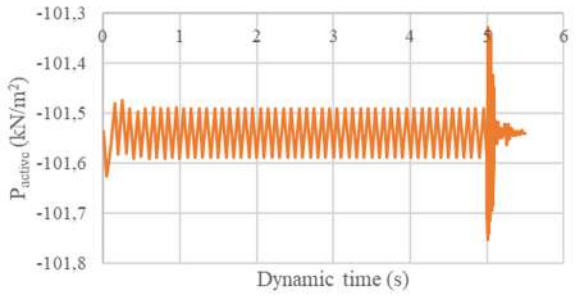

Fig. 13. Active pore water pressure at a depth of 12.5 m.

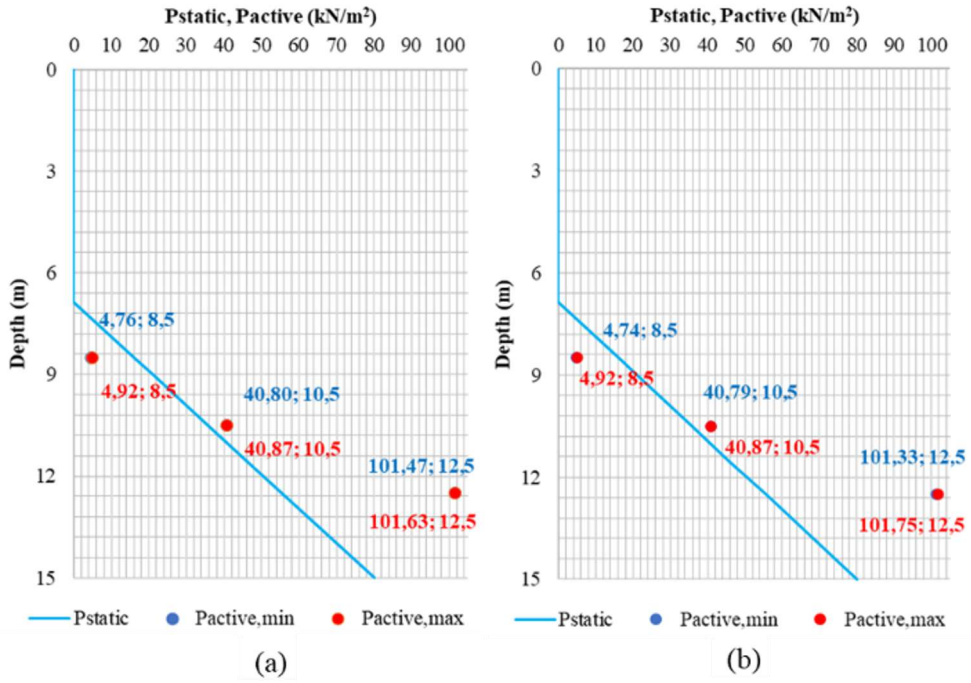

Fig. 14. Pore water pressure vs. depth: (a) dynamic load; (b) fading.

From Fig. 14, it can be seen that when the soil is dynamically loaded, the active pore water pressure of the soil is relatively greater than when it is fading. In addition, it can also be seen that the change in pore water pressure (Δ_u) tends to be greater because it is an end-bearing pile, so that the pile load will be concentrated in the end area. The liquefaction potential can also be determined by first calculating the effective circumferential stress (σ_3') per layer using Equation 1. Then, the liquefaction potential at the point under review can be identified, as shown in Tables 7-8.

Table 7. Liquefaction potential.

Depth (m)	**γ_{sat} (kN/m³)**	**σ_1 (kPa)**	**P_w (kPa)**	**σ_1' (kPa)**
0	22	0	0	0
6.85	22	150.7	0	150.7
6.85	22	150.7	0	150.7
8.5	**22**	**187**	**16.19**	**170.81**
9	22	198	21.09	176.91
9	18	198	21.09	176.91
10.5	**18**	**225**	**35.81**	**189.19**
11.55	18	243.9	46.11	197.79
11.55	20	243.9	46.11	197.79
12.5	**20**	**262.9**	**55.43**	**207.47**
15	20	312.9	79.95	232.95

Based on **Table 7** the value of the ratio of pore water pressure (r_u) is less than 1, which means that it can be concluded that in the three layers of soil observed, especially sandy soils in the first and third layers, there are increments of excess pore water pressure but liquefaction state has not occurred. This phenomenon can reduce the bearing capacity of the foundation piles because the effective stress will decrease.

Table 8. Liquefaction potential.

Depth (m)	k_0	σ_3' (kPa)	U_{excess} (kPa)	$r_u = U_{excess}/\sigma_3'$	Liquefaction Potential
0.00	0.39	0			
6.85	0.39	58.95			
6.85	0.39	58.95			
8.50	**0.39**	**66.82**	**21.42**	**0.32**	**No**
9.00	0.39	69.21			
9.00	1.00	176.91			
10.50	**1.00**	**189.19**	**4.29**	**0.02**	**No**
11.55	1.00	197.79			
11.55	0.39	77.38			
12.50	**0.39**	**81.16**	**44.83**	**0.49**	**No**
15.00	0.39	91.13			

3.2 Pile capacity analysis

As a result of excess pore water pressure on saturated sand soils, leads to reduced skin capacity which can be calculated in the following ways (data can be seen in Tables 9-12).

Without Reduction:

$Q_{s,total} = \sum A_s f$
$= (12.91 \times 11.01) + (4.05 \times 24.03) + (4.81 \times 45.90) + (8.39 \times 43.61)$
$=$ **1,007.68** kN

With Reduction:

$Q_{s,total} = \sum A_s f_{reduction}$
$= (12.91 \times 21.59) + (4.05 \times 47.12) + (4.81 \times 45.90) + (8.39 \times 64.13)$
$=$ **605,36** kN

The end bearing capacity is calculated at a depth of 4D ($4 \times 0{,}6 = 2{,}4$ m ≈ 3 m) from the pile toe as follows (data can be seen in the Table 13).

Table 9. Foundation skin capacity in sand (β Method).

Elevation (m)		ΔL (m)	γ' (kN/m³)	σ'₀ (kN/m²)	φ' (°)	K
0	6.85	6.85	21	71.925	37.5	0.4
6.85	9	2.15	12.19	156.95	37.5	0.4
9	11.55	2.55	8.19	180.501	-	-
11.55	16	4.45	10.19	213.616	37.5	0.4

Table 10. Foundation skin capacity in sand (β Method).

Elevation (m)		β	f (kPa)	$f_{reduction}$ (kPa)	A_s (m²)
0	6.85	0.3	21.59	11.01	12.91
6.85	9	0.3	47.12	24.03	4.05
9	11.55	-	-	-	-
11.55	16	0.3	64.13	43.61	8.39

Table 11. Foundation skin capacity in clay (α Method).

Elevation (m)		ΔL (m)	γ' (kN/m³)	σ'₀ (kN/m²)	c_u (kN/m²)
0	6.85	6.85	21	71.93	-
6.85	9	2.15	12.19	156.95	-
9	11.55	2.55	8.19	180.50	90
11.55	16	4.45	10.19	213.62	-

Table 12. Foundation skin capacity in clay (α Method).

Elevation (m)		C_u/ ($P_a \approx 100$ kN/m²)	α	f (kPa)	A_s (m²)
0	6.85	‘	-	-	-
6.85	9	-	-	-	-
9	11.55	-	0.51	45.90	4.81
11.55	16	-	-	-	-

Table 13. Foundation end bearing capacity.

Elevation (m)		Depth (m)	N-SPT (*blows /feet*)	α	N_b (*blows /feet*)	K_b	A_p (m²)	Q_p (kN)
13	14	1	25	1	4.167	325	0.28	382.88
14	15	1	50	1	8.333	325	0.28	765.76
15	16	1	50	1	8.333	325	0.28	765.76
16	17	1	50	1	8.333	325	0.28	765.76
17	18	1	50	1	8.333	325	0.28	765.76
18	19	1	50	1	8.333	325	0.28	765.76
Total		6	275		45.8333			**4211.70**

However, the soil bearing capacity should not exceed of the following allowable material stress limit:

$Q_{p,allowable} = ¼ \times A_p \times f'_c$
$= ¼ \times 0{,}28 \times 52$
$=$ **3,675.66** kN

So, the bearing capacity of pile value is generated as follows:

Without Reduction:

$Q_u = Q_{p,total} + Q_{s,total}$
$= 3675.66 + 1007.68$
$=$ **4,903.96** kN

$Q_a = \frac{Q_u}{SF}$
$= \frac{4903.96}{2.5}$
$=$ **1,961.59** kN

With Reduction:

$Q_u = Q_{p,total} + Q_{s,total}$
$= 3675.66 + 605.36$
$=$ **4,501.65** kN

$Q_a = \frac{Q_u}{SF}$
$= \frac{4{,}501.65}{2.5}$
$=$ **1,800.66** kN

4 Conclusions

From the harmonic loading of the machine foundation modeling, several conclusions can be drawn, as follows:

1. In the first soil layer, which is below the GWL, the pore water pressure that occurs is suction, while in the second and third soil layers, the pore water pressure that occurs tends to be compressive;
2. Changes in pore water pressure (Δ_u) tend to be greater in deeper layers. Because the load distribution for end bearing pile will be concentrated around the pile’s tip;
3. The active pore water pressure of the soil is relatively smaller than when it is fading;

4. In sandy soils that have excess pore water pressure but no liquefaction, the bearing capacity needs to be reduced by considering the value of r_u. The magnitude of the multiplier for the reduction in skin capacity is about 1-r_u, 51-68 %.
5. The allowable pile bearing capacity without reduction is Q_a = 1,961.59 kN, and with reduction is Q_a =1,800.66 kN.

References

1. Bentley, PLAXIS connect edition V22.01, (Bentley Communities, 2022)
2. R.D. Holtz, W.D. Kovacs, T.C. Sheahan, An introduction to geotechnical engineering 2nd Ed. (Pearson Education, Inc., 2011)
3. B.M. Das, G. Ramana, Principles of soil dynamics 2nd Ed. (Cengange Learning, 2011)
4. S.L. Kramer, Geotechnical earthquake engineering (Prentice-Hall, Inc., 1996)
5. Canadian Geotechnical Society, Canadian foundation engineering manual 4th Ed. (2006)
6. B.M. Das, Principle of foundation engineering 8th Ed. (Cengage Learning, 2016)
7. Veronica, A. Prihatiningsih, A. Iskandar, JMTS **6**(2), 415-428 (2023) https://doi.org/10.24912/jmts.v6i2.21991